Supplementary Material for Highly Efficient and Stabe $Cs_3Mn_{0.93}Zn_{0.07}Br_5@SiO_2$ for Wide Color Gamut Backlight Displays

Chun Sun[a, b, *], Zhihui Deng[a, b], Xiaohui Liu[c, d], Fuhao Zhang[a, b], Kai Lian[a, b], Yiwei Zhao[a, b], Hu Zhang[a, b], Jiachen Han[a, b], and Mingming Luo[a, b, *]

AFFILIATIONS

[a.] State Key Laboratory of Reliability and Intelligence of Electrical Equipment, Hebei University of Technology, 5340 Xiping Road, Tianjin 300401, PR China

[b.] Tianjin Key Laboratory of Electronic Materials and Devices, School of Electronics and Information Engineering, Hebei University of Technology, 5340 Xiping Road, Tianjin 300401, PR China

[c.] Key Laboratory of Magnetism and Magnetic Materials Autonomous Region, Baotou Teachers' College, Inner Mongolia University of Science and Technology, 3 Kexue Road, Baotou, 014030, P.R. China

[d.] Zhejiang Ruico Advanced Material Co., Ltd., No.188 Liangshan Road, Huzhou, 313018, PR China.

* **E-mail:** cs@hebut.edu.cn (Chun Sun). mmluo@hebut.edu.cn (Mingming Luo).

Experimental Section

Chemicals.

The materials used were manganese acetate (98%, Aladdin), cesium acetate (99.9%, Aladdin), zinc acetate dihydrate (99.99%, Aladdin), trimethylbromosilane (99%, J&K), isopropanol (AR, MACKLIN), and tetramethoxysilane (TMOS, Aladdin, 98%). All chemicals were used directly without further purification.

Synthesis of Cs_3MnBr_5 (CMB) powders.

CMB powders were made by a simple room-temperature synthesis method.[1] Then, 0.35 mmol of manganese acetate and 0.1 mmol of cesium acetate were added to 15 ml of isopropanol, and ultrasonicated for 6 h until completely dissolved. Then, 150 μl of trimethylbromosilane was added to the above precursor solution. After ultrasonic treatment for 1 h, the CMB powders were obtained from the centrifuge reaction mixture.

Synthesis of $Cs_3Mn_{(1-x)}Zn_xBr_5@SiO_2$ (CMZBS) powders.

The $Cs_3Mn_{(1-x)}Zn_xBr_5$ (CMZB) powders were synthesized by the same method, just adding zinc acetate dihydrate with different molar ratios ([Zn]/[Mn]=0:1, 0.01:1, 0.03:1, 0.05:1, 0.07:01, 0.1:1) to the precursors of cesium acetate and manganese acetate. Until the powder was completely dissolved, trimethylbromosilane was added to continue to ultrasonicate. After ultrasonic treatment for 1 h, a different amount of TMOS was added and stirred for 12 h. Finally, the CMZBS powders were obtained from the

centrifuge reaction mixture.

First-Principle Calculations Based on DFT.

The formation energies for $Cs_3Mn_{(1-x)}Zn_xBr_5$ were evaluated using the DFT plane-wave pseudopotential method as implemented in the CASTEP module integrated in the Material Studio 2018. The exchange-correlation effects were treated by the generalized gradient approximation with Perdew–Burke–Ernzerhof (GGA-PBE) and the OTFG ultrasoft pseudopotentials were employed for all calculations. Energies were performed using a 2 × 2 × 1 supercell containing 32 unit cells with a energy cutoff of 500 eV and k-points of 6 × 6 × 4. The structures were fully relaxed until the convergence of total energy on each atom were less than 10^{-6} eV.

Characterization.

X-ray diffraction (XRD, Bruker D8 ADVANCE X, Germany) was used to carry out structure characterization, operating at 4 kV and 100 mA with monochromatized Cu Kα radiation (λ = 1.5406 Å). Both photoluminescence excitation (PLE) and photoluminescence (PL) were measured by an Edinburgh FLS920 fluorescence spectrometer. The PLQY and temperature-dependent PL spectrum (temperature ranges from 293 K to 433 K, step temperature is 20 K) were measured by a fluorescence spectrometer (FLS920P, Edinburgh Instruments). Fourier transform infrared (FTIR) spectroscopy was conducted on a Thermo-Nicole iS50

FTIR spectrometer. Scanning electron microscopy (SEM, Hitachi S-4800) was used to characterize the surface morphology of the sample, and EDS mapping was used to obtain the actual element distribution image. Transmission Electron Microscope(TEM, FEI-Themis G2 300) was used to measure the thickness of SiO_2. X-ray photoelectron spectroscopy (XPS, PHI5000 Versaprobe Ⅲ) was used to analyze changes in chemical element content and binding energy.

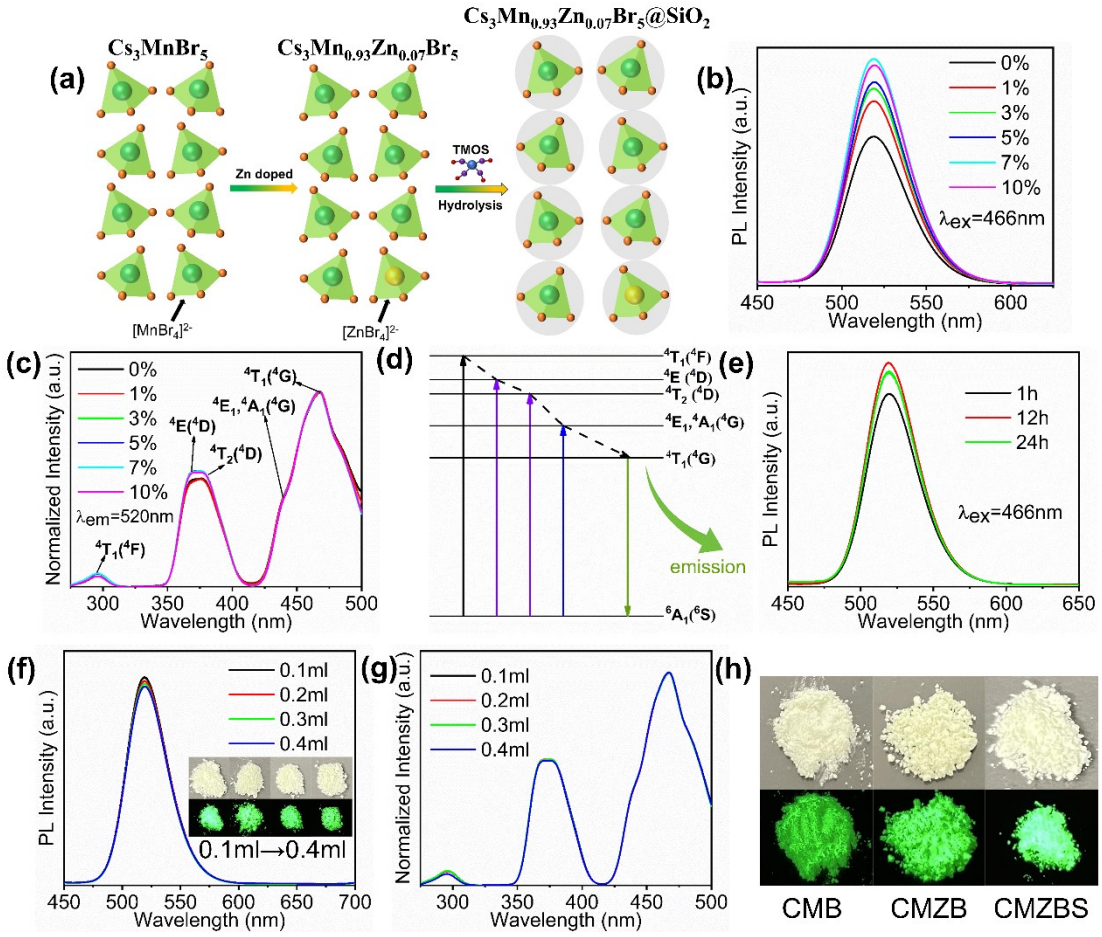

Figure S1. (a) Schematic showing the synthesis of CMZBS. PL (b) and PLE (c) spectra

of $Cs_3Mn_{(1-x)}Zn_xBr_5$ (x = 0, 0.01, 0.03, 0.05, 0.07, 0.09, and 0.1). (d) Schematic diagram of the PL mechanism. (e) PL spectra of CMZB with 0.1 ml TMOS hydrolysis at different times. (f) PL spectra of different TMOS amounts for hydrolysis at 12 h, inserted with the images of CMZBS under fluorescent lamps (up) and ultraviolet lamps (down). (g) PLE spectra of CMZB with different amounts of TMOS hydrolysis at 520 nm. (h) Photos of CMB (left), CMZB (middle), and CMZBS (right) under fluorescent lamps (top) and 365 nm ultraviolet lamps (bottom).

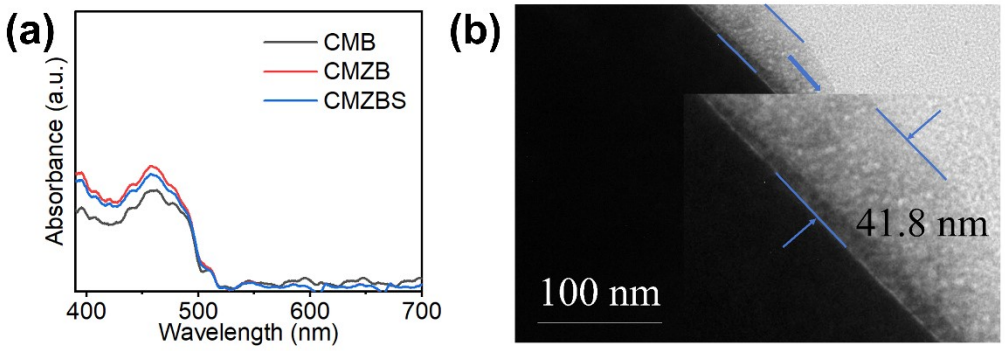

Figure S2. (a) The absorption spectra of CMB, CMZB, and CMZBS. (b) TEM image of CMZBS.

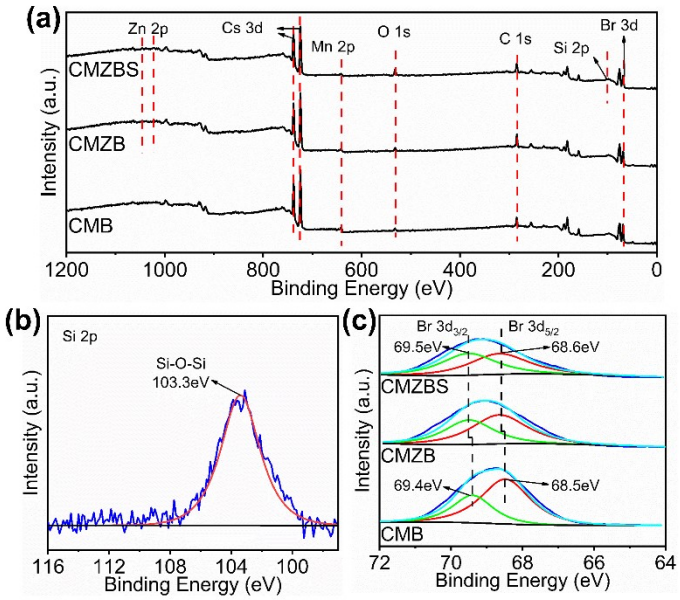

Figure S3. (a) XPS spectra of CMB, CMZB, and CMZBS. (b) XPS spectrum of Si 2p for CMZBS. (c) XPS spectra of Br 3d for CMB, CMZB, and CMZBS.

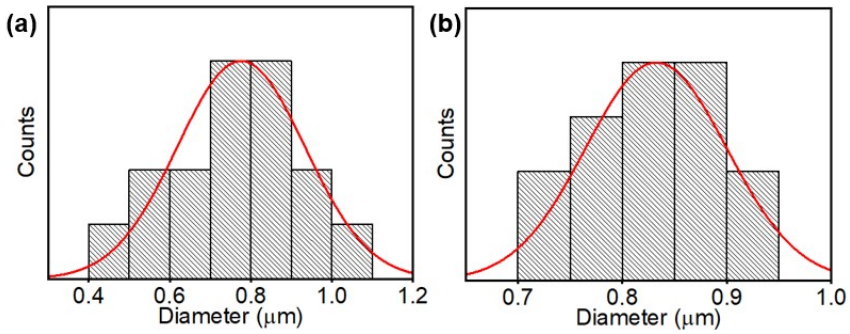

Figure S4. The corresponding size distribution of CMZB (a), and CMZBS (b) in the specimen

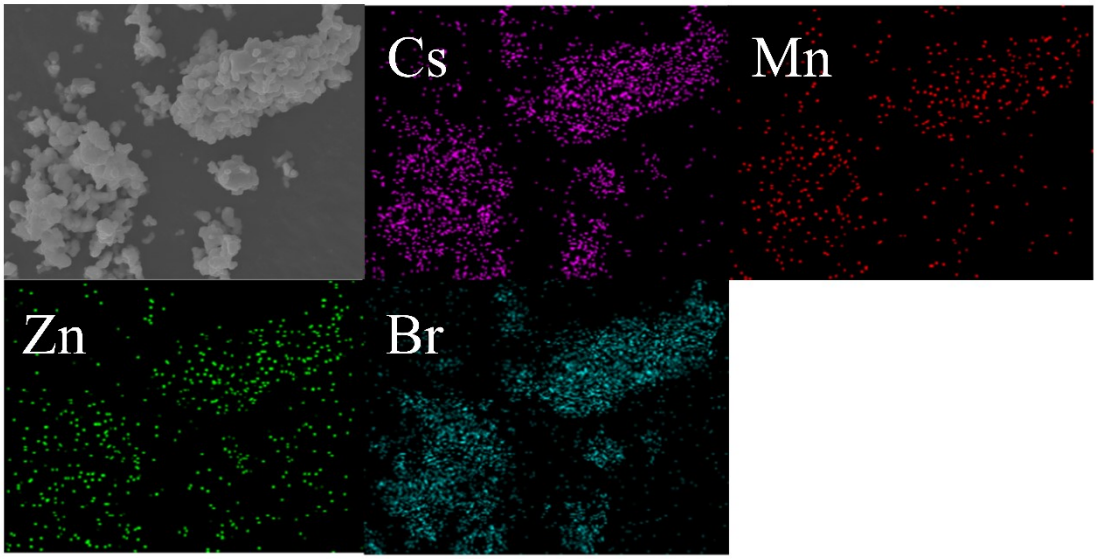

Figure S5. SEM and EDS mapping image of CMZB to identify the element distribution of Cs, Mn, Br, and Zn.

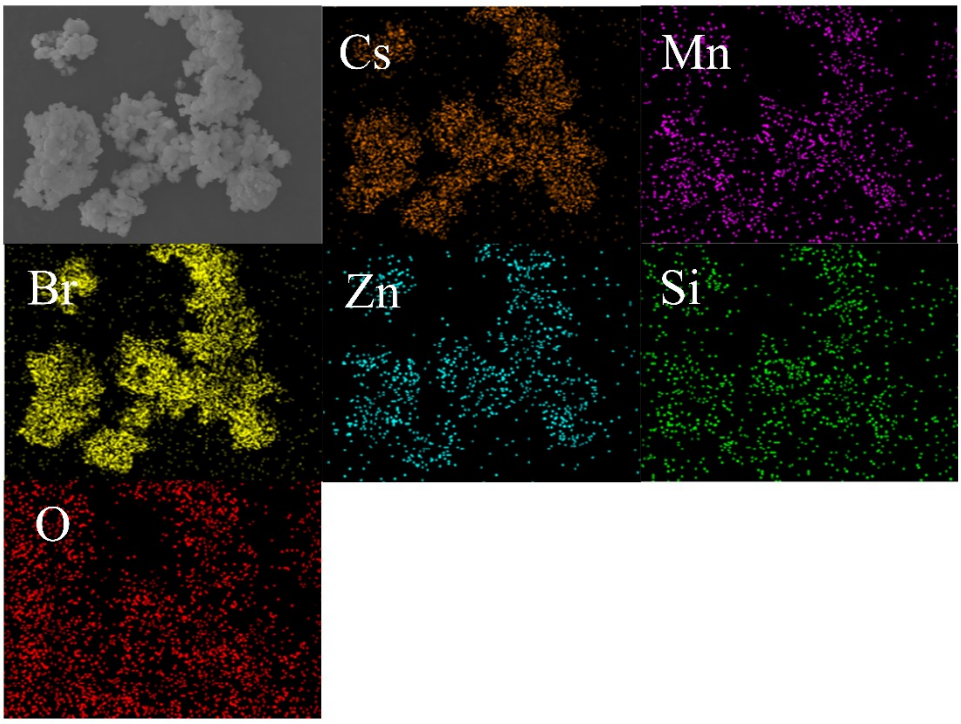

Figure S6. SEM and EDS mapping images of CMZBS to identify the element distribution of Cs, Mn, Zn, Br, Si, and O.

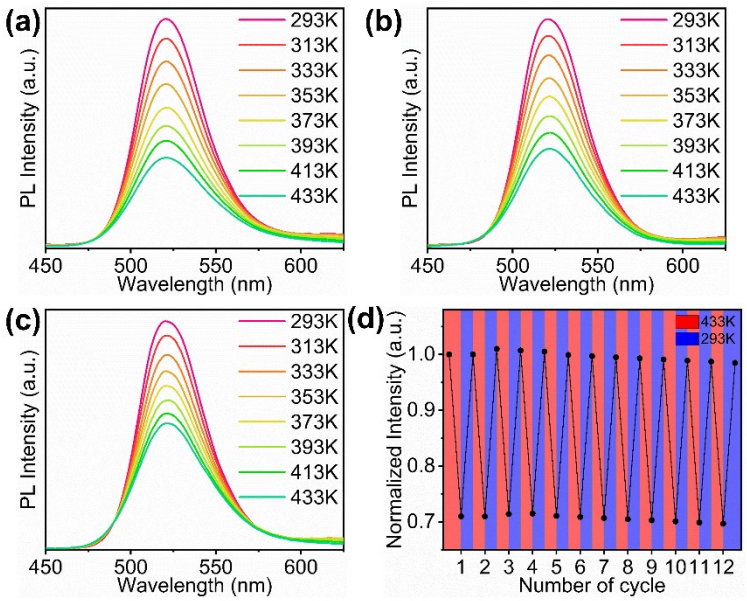

Figure S7. Temperature-dependent PL spectra of CMB (a), CMBS (b), and CMZB (c) under 365 nm in the temperature range of 293 K–423 K. (d) The heating and cooling cycle test of CMZBS between 293 and 433 K.

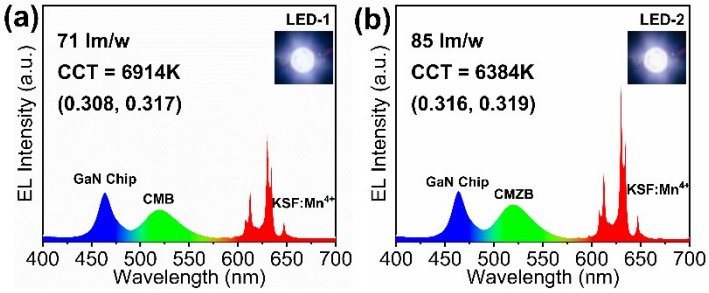

Figure S8. EL spectra of the WLED devices fabricated with different green phosphor CMB (a), CMZB (b), and red phosphor KSF:Mn^{4+} on a blue LED GaN chip (465 nm) under a current of 20 mA. The inset shows the photos of lightened WLEDs.

Table S1. The PLQY comparison of CMB, CMZB, and CMZBS.

	PLQY (%)

CMB	CMZB	CMZBS
51	72	80

Table S2. The ratio of elements in the products of CMB, CMZB, and CMZBS detected by XPS.

Samples	atomic ratio (%)					
	Cs	Mn	Zn	Br	Si	O
CMB	26.89	10.76	0	62.35	0	0
CMZB	27.59	10.86	0.79	60.76	0	0
CMZBS	23.71	6.02	0.39	42.85	8.68	18.35

Table S3. The ratio of elements in the product of CMZB detected by EDS

EDS (atomic ratio %)					
Cs	Mn	Zn	Br	Si	O
32.17	10.07	0.84	54.95	0	1.97

Table S4. The ratio of elements in the product of CMZBS detected by EDS

EDS (atomic ratio %)					
Cs	Mn	Zn	Br	Si	O
27.25	8.43	0.66	45.92	5.46	12.28

Table S5. Calculated Formation Energies (ΔH_f) for Cs_3MnBr_5 doped with different ratios of Zn^{2+} by Using First-Principle Calculations Based on DFT.

crystal	Zn content (%)	ΔH_f (eV)
Cs_3MnBr_5	0	-6.21
$Cs_3Mn_{0.95}Zn_{0.05}Br_5$	5	-6.60
$Cs_3Mn_{0.9}Zn_{0.1}Br_5$	10	-6.81
$Cs_3Mn_{0.85}Zn_{0.15}Br_5$	15	-6.75
$Cs_3Mn_{0.8}Zn_{0.2}Br_5$	20	-6.47

Table S6. Comparison of the PLQY and thermal stability of different posttreatment methods.

Green phosphor	PLQY	Thermal stability	Ref
$Cs_3Mn_{0.96}Zn_{0.04}Br_5$	49%	87% at 423 K	[2]
$CsMnBr_3NCs$@glass	66%	81% at 373 K	[3]
$Cs_3Mn_{0.6}Zn_{0.4}Br_5$@PS	43%	50% at 423 K	[4]
$Cs_3MnZnBr_5$@glass	50%	65% at 448 K	[5]
$Cs_3Mn_{0.93}Zn_{0.07}Br_5@SiO_2$	80%	71% at 433 K	This work

REFERENCES

1 P. Gao, S. Cheng, J. Liu, J. Li, Y. Guo, Z. Deng, T. Qin and A. Wang, *Molecules*, 2022, **27**.
2 B. Su, M. S. Molokeev and Z. Xia, *J. Mater. Chem. C*, 2019, **7**, 11220-11226.
3 G. Xu, C. Wang, Y. Li, W. Meng, G. Luo, M. Peng, B. Xu and Z. Deng, *Chem. Sci.*, 2023, **14**, 5309-5315.
4 W. Chen, Q. He, Z. He, Q. Wang, J. Ding, Q. Huang, X. Liang, Z. Chen and W. Xiang, *ACS Sustainable Chem. Eng.*, 2022, **10**, 5333-5340.
5 K. Li, Y. Ye, W. Zhang, Y. Zhang and C. Liu, *Inorg. Chem.*, 2023, **62**, 13001-13010.